Available online at www.sciencedirect.com

SCIENCE DIRECT®

Materials Letters 59 (2005) 3795 – 3800

materials letters

www.elsevier.com/locate/matlet

# Production of TiC reinforced-aluminum composites with the addition of elemental carbon

Isıl Kerti

*Department of Metallurgical and Materials Engineering, Faculty of Chemistry & Metallurgy, Yıldız Technical University, Davutpasa Campus, Esenler, Istanbul, Turkey*

Received 6 May 2005; accepted 23 June 2005
Available online 8 August 2005

**Abstract**

TiC reinforced Al matrix composites were produced by the additions of elemental carbon to both Al+4%Ti and Al+5%Ti alloys. It is shown that the microstructure, phase composition as well as fracture behavior of the composites produced are controlled by the processing parameters, such as temperature, amount of excess carbon and duration. Composite microstructure subjected to 1300 °C for 15 min includes only TiC particles where the fracture occurs in a ductile manner whilst composites subjected to 1200 °C for 30 min contain $Al_3Ti$ and TiC particles which show mixed mode of fracture behavior where $Al_3Ti$ particles resulted in brittle fracture due to their coarser size.
© 2005 Elsevier B.V. All rights reserved.

*Keywords:* In situ production; Composite materials; Aluminum composites; TiC

## 1. Introduction

Today searches in finding new materials superior than the conventional ones have an increasing demands. In these studies, aluminum based composite materials have been taking great attention especially in the industries such as aviation, space, and automotive [1]. The superiority of aluminum matrix composite materials over conventional ones is their high strength, high elastic modules, excellent friction and wear resistance and low heat expansion coefficients [2]. TiC is used as reinforcement phase because of its high hardness and elastic modules, low density, good wettability with molten aluminum and its low chemical reactivity [3].

There are various in situ production methods for TiC reinforced aluminum based composites such as exothermic dispersion (XD™), reaction gas injection, self propagating high-temperature synthesis (SHS), liquid–solid reactions and liquid–liquid reactions [4–8].

In addition to these methods, it is likely to produce TiC reinforced Al based composites with the help of elemental carbon, graphite or amorphous carbon [9]. Therefore, carbon addition is one of the new methods for the production of TiC reinforced aluminum composites where graphite or amorphous carbon can be used as elemental carbon source. At elevated temperatures carbon reacts with Al–Ti melt and produces TiC which acts as reinforcement phase.

The stability of $Al_4C_3$ and TiC phases in aluminum melt depends on their free energies. As C added into Al–Ti melt, Ti and C dissolve and react to form TiC.

Possible reactions and their free energies in Al–Ti–C system are given below [10];

$$\mathrm{Ti} + \mathrm{C} \rightarrow \mathrm{TiC} \qquad \Delta G = -186606 + 13.22T \text{ J mol}^{-1} \quad (1)$$

$$4/3\ \mathrm{Al} + \mathrm{C} \rightarrow 1/3\ \mathrm{Al_4C_3}$$
$$\Delta G = -88840 + 32.1T \text{ J mol}^{-1} \quad (2)$$

As stated in the literature, transformation free energy for one mole TiC is lower than that of $Al_4C_3$, therefore it can be concluded that thermodynamically TiC is more stable than $Al_4C_3$ [8,11].

*E-mail address:* ckerti@yildiz.edu.tr.

0167-577X/$ - see front matter © 2005 Elsevier B.V. All rights reserved.
doi:10.1016/j.matlet.2005.06.032

Table 1
Chemical composition of the materials used

| Alloys | % Al | % Fe | % Si | % Cu | % Ti | % Zn | Diğerleri |
|---|---|---|---|---|---|---|---|
| Al+6%Ti | 92.88 | 0.157 | 0.148 | 0.003 | 6.350 | 0.097 | 0.100 |
| Etial8 | 99.80 | 0.150 | 0.100 | 0.030 | 0.008 | 0.020 | 0.100 |

Table 2
Composition of the materials used and experimental conditions for composite processing

| Sample no. | Composition | Excess C (wt.% ) | Reaction temperature (°C) | Holding time (min) |
|---|---|---|---|---|
| 1 | Al+4%Ti | 20 | 1200 | 15 |
| 2 | Al+4%Ti | 30 | 1200 | 15 |
| 3 | Al+4%Ti | 30 | 1300 | 15 |
| 4 | Al+5%Ti | 20 | 1200 | 15 |
| 5 | Al+5%Ti | 30 | 1300 | 5 |
| 6 | Al+5%Ti | 30 | 1300 | 15 |

The advantages of this method to other methods in which a reinforcement phase nucleates in Al matrix, are easy of production, no need for sophisticated production technology, the low production cost, no wettability problem which is seen in other production methods, no contamination in between matrix-reinforced phase which lowers mechanical properties.

Therefore, in the present work the effects of excess carbon, reaction temperature and duration on the microstructure and phase composition of Al–4%Ti and Al–5%Ti composites were investigated by SEM observations and detail XRD analysis.

## 2. Experimental procedure

Al+6%Ti master alloy and commercial purity (CP) AA[1080] are supplied by London Scandinavian Metallurgy (LSM) and Seydi°ehir Eti Alüminyum, respectively. The chemical compositions of both materials are given in Table 1. As elemental carbon, Elftex125 Cabot with average particle size of 10–20 μm is used.

Various Al–Ti alloys having different chemical compositions were melted in a pure alumina coated graphite crucible utilizing induction furnace. Melt temperature is raised to 1200 °C and held for 30 min to dissolve $Al_3Ti$ phase completely.

Carbon with an average particle size of 10–20 μm is first dried at 850 °C to eliminate humidity. Pre heated 1 g carbon particles are packed in aluminum foils and added into crucible, then temperature is raised to the reaction temperature and kept there until the full reaction takes place.

All the experimental variables including composition of master alloy, the amount of carbon, temperature and duration are given in Table 2.

After the completion of casting process, Al based TiC reinforced composites were subjected to rolling operation at 400 °C. Three passes and 80% reduction are applied during rolling. Samples taken from rolled materials are prepared for microstructural investigations. After grinding and polishing, samples were etched in Keller's reagent.

A series of XRD analyses has been made on materials using Philips PW1820 with CuKα (1.54 Å) and CoKα ($\lambda = 1.7$) at diffraction angles $2\theta = 35–80°$. The particle size distribution of carbon is measured by Malvern master sizer. For microstructural investigations Jeol JSM 5410LV scanning electron microscope is employed. In order to determine the volume ratio in the products Leica MPS 60 analyzer is employed.

## 3. Results and discussion

The effect of temperature on the formation of TiC in Al–4%Ti alloy has been shown in XRD spectrums (Fig. 1). In the samples

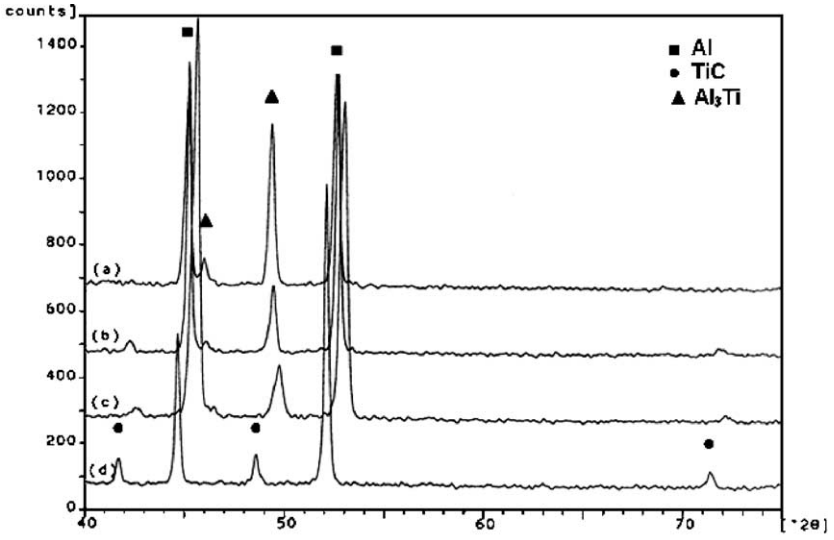



Fig. 1. XRD traces of (a) Al–4%Ti alloy, (b) sample no. 1, (c) sample no. 2, and (d) sample no. 3 shown in Table 2.

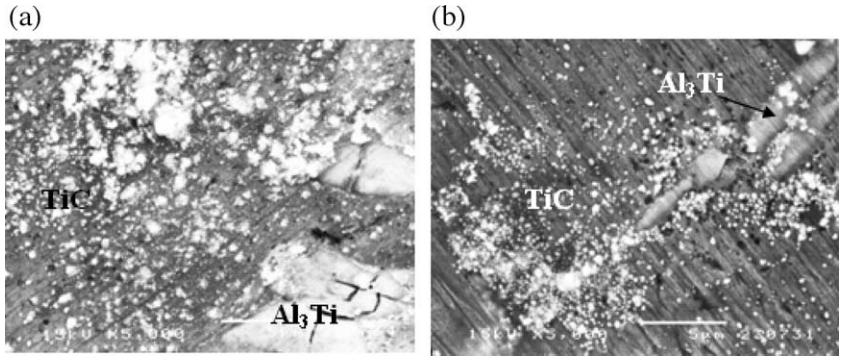



Fig. 2. SEM micrographs of the sample (a) no. 1 and (b) no. 2 indicating the presence of both TiC and $Al_3Ti$ phases.

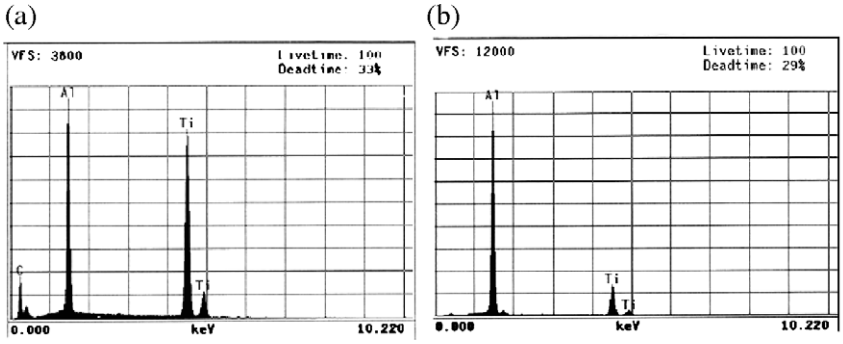



Fig. 3. EDS analysis of sample nos. (a) 1: Ti and C peaks belong to TiC particles which were shown in Fig. 2(a) as fine homogeneously distributed phases, (b) 2: Ti and Al peaks belong to $Al_3Ti$ particles with a size of 10 μm and as shown in Fig. 2(b).

no. 1, 2 and 3 which have 20%, 30% and 30% excess carbon and held for 15 min at 1200 °C, $Al_3Ti$ and TiC peaks were found along with aluminum. This result clearly illustrates that the experimental conditions for the transformation of TiC were not suitable. The reason for this incomplete transformation of TiC is that the duration for full transformation was not sufficient at 1200 °C and under these experimental conditions carbon was not wetted by Al–Ti melt. This result is in good agreement with the findings of N. Sobczak et al. [12] who find that with increasing temperature and time wetting angle decreases below 90°. From this concept, it can be contributed that in order to obtain an ideal wetting angle the reaction temperature should be increased. The SEM micrographs and EDS results of samples no. 1 and 2 are shown in Figs. 2 and 3, respectively whilst the microstructure of sample 3 is shown in Fig. 4.

It was determined from the SEM pictures presented in Fig. 2(a) and (b) that along with 1 μm TiC particles, $Al_3Ti$ particles with an average size of 10 μm form within the structure under the experimental conditions used for the samples no. 1 and 2. Presence of both TiC and $Al_3Ti$ particles were confirmed by EDS analysis as shown in Fig. 3(a) and (b). However when the XRD trace of sample no. 3 which was processed at 1300 °C is analyzed, it shows that although the chemical composition of this alloy is the same with that of both samples of 1 and 2, $Al_3Ti$ phase was disappeared (Fig. 1). This result was also confirmed by the SEM observation as shown in Fig. 4. After the addition of 30% excess carbon at 1300 °C for 15 min all of $Al_3Ti$ phases transform to TiC.

The effect of carbon addition above stoichiometric ratio and duration on the formation of TiC in Al+5%Ti alloy has also been investigated. As shown in XRD spectrum in Fig. 5, with increasing temperature and carbon addition, the intensity of $Al_3Ti$ peaks is seen to decrease. After 15 min at 1300 °C, in samples 4 and 5 which have 20% and 30% excess carbon, respectively, XRD trace shows Al and $Al_3Ti$ peaks in Fig. 5. In both samples of numbers 4 and 5, with 20% and 30% excess carbon contents and subjected to 1300 °C for 5 min, respectively, TiC peaks along with Al and $Al_3Ti$ are present as illustrated in Fig. 5.

The SEM microstructures of sample nos. 4 and 5 clearly show the presence and homogeneous distribution of TiC particles within the microstructure as well as $Al_3Ti$ phase as shown in Fig. 6(a) and (b), respectively.

Sample no. 6 with 30% excess carbon which was subjected to 1300 °C for 15 min shows only TiC phase homogenously

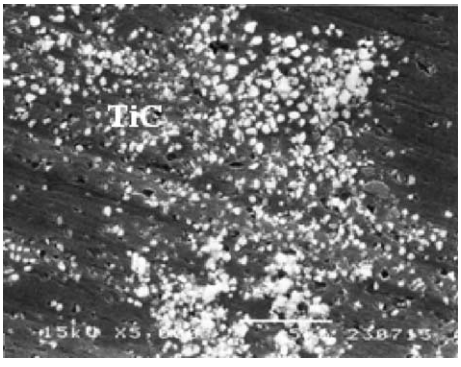



Fig. 4. SEM micrograph of the sample no. 3 showing full transformation of $Al_3Ti$ to TiC at 1300 °C for 15 min.

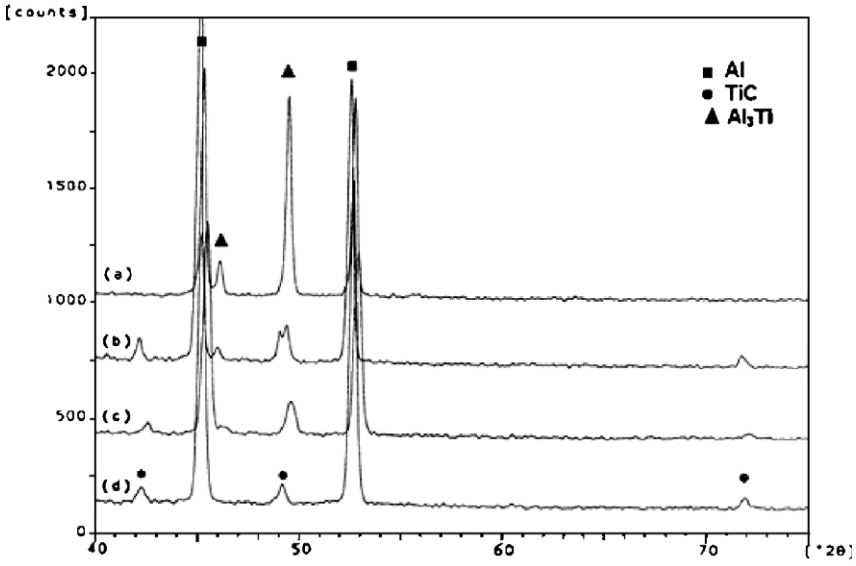



Fig. 5. XRD traces of samples of (a) Al–5%Ti alloy, (b) no. 4, (c) no. 5, and (d) no. 6 shown in Table 2.

distributed within the microstructure as the XRD results and SEM micrographs are presented in Figs. 5 and 6(c), respectively.

In samples 3 and 6 where TiC formation was completed, the volume fraction of TiC has been determined using an image analyzer connected to SEM and it was found that in both samples the volume fraction of TiC was about 15%.

In order to see the effect of TiC formation on fracture surfaces, Al+4%Ti with no addition of excess carbon, sample no. 2 which contains both TiC and $Al_3Ti$ particles and sample no. 3 which contains only TiC particles were investigated and the results are presented in Fig. 7(a)–(d), respectively.

As shown in Fig. 7(a), brittle fracture is seen in the sample with no excess carbon addition. However, in fracture surface of sample no. 2 which contains both TiC and $Al_3Ti$ phases, some areas where small size TiC particles present show ductile fracture behavior and areas that contain coarser $Al_3Ti$ particles fracture in a brittle manner as shown in Fig. 7(b).

The fracture surface of sample no. 3, which has the complete transformation of TiC, has shown ductile fracture behavior as

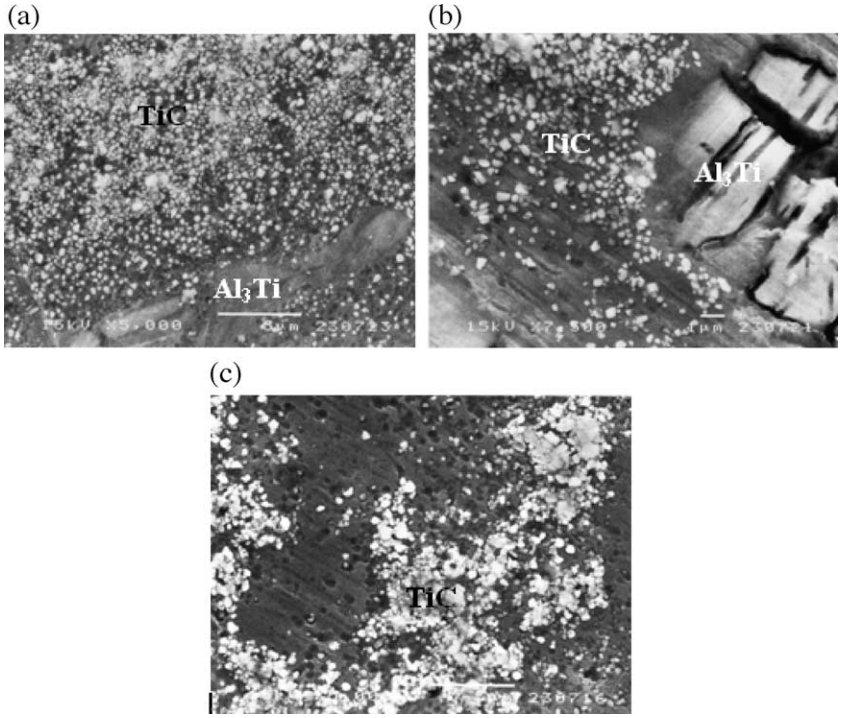



Fig. 6. SEM pictures of sample nos. (a) 4, (b) 5, showing the presence of both TiC and $Al_3Ti$ and (c) 6 showing only TiC phase within the structure at 1300 °C for 15 min.

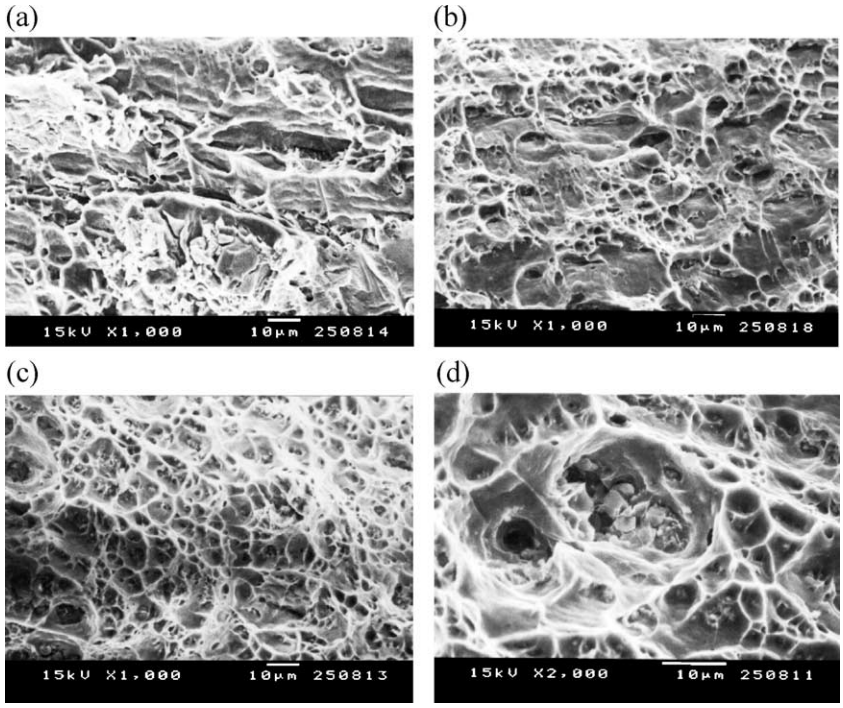



Fig. 7. Fracture surfaces of samples (a) Al+4%Ti alloy, (b) no. 2, (c) no. 3 and (d) no. 3.

shown in Fig. 7(c). No decohesion was observed between 1 μm size TiC and matrix, as shown in detail fracture surface in Fig. 7(d) and there was a very powerful bond between TiC and matrix. However, in case of particles larger than 2 μm decohesions were seen as shown in Fig. 7(d). These results are in good agreement with the findings of Sahoo and Koczak [13].

When the XRD results were combined with the microstructural examinations, our findings were in a good agreement with the published theories in the literature. As very well known, in ductile materials, fracture occurs in three stages: nucleation, growth and propagation. These stages are affected by the size of particles and their volume fractions. In simple porosity growth model, Sahoo and Koczak [13] assert that in the direction of load when pore height grows as the distance of pores a connection occurs among pores. As the fraction of reinforcement particles increases, the distance among particulates decreases and therefore, the risk of failure reduces. In case of ductile materials having hard reinforcement particles, failure nucleation affects final ductility. Ductility increases with decreasing particle size. Having coarser particles in composite materials lowers the ductility of composite materials. The presence of coarser $Al_3Ti$ particles failure nucleation starts with particle fracture.

## 4. Conclusions

TiC reinforced Al matrix composites were produced by the additions of elemental carbon to both Al+4%Ti and Al+5%Ti alloys and the following findings are concluded;

- In elemental carbon addition method, TiC forms between the reaction of carbon and Ti in solution.
- In both Al+4%Ti and Al+5%Ti, with the addition of 30% excess carbon at 1300 °C for a duration time of 15 min $Al_3Ti$ phase disappears and completely transforms to TiC particles having less than 1 μm size.
- Both $Al_3Ti$ and TiC particles were determined within the microstructure subjected to 1200 °C for 30 min indicating uncompleted transformation of $Al_3Ti$ under these conditions.
- Fracture surface analysis indicates that regions where small size TiC particles (smaller than 1 μm) heavily located show ductile fracture behavior whilst areas that contain coarser $Al_3Ti$ particles (about 5 μm) indicate brittle fracture.
- There is no decohesion for the composites having 1–2 μm TiC particles. However, particles larger than 2 μm shows decohesion.

## References

[1] I. Tsunemichi, M. JianFu, D. Shangli, S. Ichinori, S. Naobumi, L. Gilles, Mater. Sci. Eng., A Struct. Mater.: Prop. Microstruct. Process. 364 (2004) 281.
[2] M.J. Koczak, M.K. Premkumar, JOM (1993 January) 44.
[3] P. Li, E.G. Kandalova, V.I. Nikitin, A.G. Makarenko, A.R. Luts, Z. Yanfei, Scr. Mater. 49 (2003) 699.
[4] A.R.C. Westwood, Metall. Trans., A, Phys. Metall. Mater. Sci. 19A (1998 April) 749.
[5] R. Mitra, W.A. Chiou, M.E. Fine, J.R. Weertman, J. Mater. Res. 8 (9) (1993 Sep.) 2380.
[6] M.J. Koczak, M.K. Premkumar, JOM (1993 January) 44–48.
[7] M.J. Koczak, K.S. Kumar, U.S. Patent 4, 808, 372, 1989.
[8] P. Sahoo, M.J. Koczak, Mater. Sci. Eng., A Struct. Mater.: Prop. Microstruct. Process. 144 (1991) 37.

[9] A. Banerji, W. Raif, Metall. Trans., A, Phys. Metall. Mater. Sci 17A (1986) 2127.
[10] S. Khatri, M.J. Koczak, Mater. Sci. Eng., A Struct. Mater.: Prop. Microstruct. Process. 162 (1993) 153.
[11] R.A. Rapp, X. Zheng, Metall. Trans., A, Phys. Metall. Mater. Sci 22A (1991 December) 3071.
[12] N. Sobczak, Z. Gorny, M. Ksiazek, W. Radziwıill, P. Rohatgi, Mat. Sci. Forum 217–222 (1996) 153.
[13] P. Sahoo, M.J. Koczak, Mater. Sci. Eng., A Struct. Mater.: Prop. Microstruct. Process. 131 (1991) 69.